Positron scattering by the negative hydrogen ion

Mary T. McAlinden,[1] Jennifer E. Blackwood,[2] and H. R. J. Walters[2]
[1]*School of Computing and Mathematical Sciences, Oxford Brookes University, Wheatley Campus, Oxford OX33 1HX, United Kingdom*
[2]*Department of Applied Mathematics and Theoretical Physics, Queen's University, Belfast BT7 1NN, United Kingdom*
(Received 10 September 2001; published 20 February 2002)

Results are presented for e^+ scattering by H^- in the impact energy range $0 \leqslant E_0 \leqslant 10$ eV. These include integrated cross sections for Ps formation in the $1s$, $2s$, and $2p$ states, as well as in an aggregate of states with $n \geqslant 3$, and for direct ionization. Differential cross sections for Ps formation in the $1s$, $2s$, and $2p$ states are also exhibited. The calculations are based on a coupled pseudostate approach employing 19 Ps pseudostates centered on the e^+. It is found that Ps formation in the $2p$ state dominates that in the $1s$ or $2s$ states below 8 eV, that formation in states with $n \geqslant 3$ exceeds the sum of the $n=1$ and $n=2$ cross sections above 2.5 eV, and that direct ionization outstrips total Ps formation above 6.3 eV. The threshold law ($E_0 \to 0$) for exothermic Ps formation, which includes the cases Ps($1s$), Ps($2s$), and Ps($2p$), is shown to be $1/E_0$.

DOI: 10.1103/PhysRevA.65.032715 PACS number(s): 34.85.+x, 95.30.Ky

I. INTRODUCTION

Positron (e^+) scattering by the negative hydrogen ion (H^-) is of interest for several reasons. First, it is the prototype of all positron-negative ion scattering reactions. Second, it is an important channel [1] of the fundamental four-body system Ps+H which is presently receiving much attention [2,3] as a result of recently acquired experimental capability to make positronium (Ps) beams [4]. Third, it is of astrophysical importance in that the reaction

$$e^+ + H^- \to Ps + H \tag{1}$$

should be a noticeable contributor to observed electron-positron annihilation linewidths in transition regions of planetary nebulas where there is a significant concentration of H^- ions [5–7]. Fourth, the development of ion storage rings which has led to a breakthrough in the study of electron-negative ion scattering [8] brings much closer the day when measurements of positron-negative ion scattering become feasible. Finally, the radiative recombination reaction,

$$e^+ + H^- \to PsH + \gamma \tag{2}$$

is, in principle, a possible route for the production of the exotic compound positronium hydride (PsH) [5,7].

We are aware of only two other papers which calculate e^+ scattering by H^- [6,9]. Both calculations are perturbative in approach and restrict themselves to Ps formation in the $1s$ ground state leaving the H atom also in its $1s$ ground state, see Eq. (1). In [9] the Coulomb-Born approximation (CBA) was used to calculate the cross section at six incident energies between 20 and 500 eV. In [6] the CBA is again used but various ''orthogonalization'' corrections to it are also considered, results are quoted only at the four incident energies of 0.1, 0.5, 1.0, and 100 eV.

Our purpose in this paper is to study the important low-energy region from 0 to 10 eV. Our emphasis is again on Ps formation, but no longer restricted to ground-state formation, we consider Ps formation in the $1s$, $2s$, and $2p$ states, as well as in an aggregate of states from $n=3$ upwards. However, we continue to assume that the resultant H atom, see Eq. (1), is left in its ground state. It turns out, as we shall see later, that Ps formation in the $2p$ state, rather than $1s$, is dominant below 8 eV. In the energy region 0–10 eV, perturbative methods are not appropriate, so we adopt a coupled-pseudostate approach [3]. The use of pseudostates also enables us to take account of the direct ionization reaction

$$e^+ + H^- \to e^+ + e^- + H(1s), \tag{3}$$

which for impact energies above 0.755 eV, the binding energy of H^- [10], is in competition with the Ps formation process (1). We present both integrated, and for Ps formation, differential cross sections.

While the use of pseudostates in calculations of e^+ scattering by neutral atoms has been highly successful [3,11–13], their deployment in e^+ scattering by weakly bound negative ions requires some thoughtful caution, the same is true for electron scattering by such ions [14]. The difference lies in how a target electron perceives the relative importance of its interaction with its parent nucleus and fellow electrons versus its interaction with the incident projectile. Under the assumption that we are not dealing with asymptotic conditions of high-impact energies or large-impact parameters, it is the latter which is overwhelmingly dominant for weakly bound negative ions. For example, the Coulomb potential of an incident $e^\pm$ at the target nucleus exceeds the binding energy of H^- if the separation distance is less than 36 a.u. [15], by contrast, this distance is reduced to 2 a.u. in the case of a neutral H target. The ''attention'' of a weakly bound electron in a negative ion under nonasymptotic conditions is therefore very much centered upon the motion of the $e^\pm$ projectile. Consequently, a treatment based on target centered pseudostates [16] is doomed to slow convergence [14,17]. This situation is more acute for positrons than for electrons since the attractive (repulsive) interaction of a projectile e^+ (e^-) pulls (pushes) a weakly bound target electron into a stronger (weaker) interaction with it. These considerations lead us to expand the collisional wave-function Ψ in terms of pseudostates centered on the e^+, i.e., in terms of Ps pseudostates,

keeping only one H^- channel, that being the entrance channel of the e^+ incident upon the H^- bound state.

II. THEORY

We expand the collisional wave-function Ψ as

$$\Psi = F(\mathbf{r}_p)\psi^-(\mathbf{r}_1,\mathbf{r}_2) + \sum_a \{G_a(\mathbf{R}_1)\phi_a(\mathbf{t}_1)\psi_0(\mathbf{r}_2) + G_a(\mathbf{R}_2)\phi_a(\mathbf{t}_2)\psi_0(\mathbf{r}_1)\}. \quad (4)$$

Here ψ^- is the H^- bound-state wave function, ψ_0 is the $1s$ ground state of the H atom and the ϕ_a are Ps states. The vector $\mathbf{r}_i(\mathbf{r}_p)$ denotes the position vector of the ith electron (positron) relative to the nucleus of the H^- ion. The vectors $\mathbf{R}_i \equiv (\mathbf{r}_p + \mathbf{r}_i)/2$ and $\mathbf{t}_i \equiv \mathbf{r}_p - \mathbf{r}_i$ then give the Ps center-of-mass position and internal coordinate, respectively. The set ϕ_a consists of both eigenstates and pseudostates of Ps. The pseudostates are constructed so that together with the eigenstates they diagonalize the Ps Hamiltonian

$$H_{\mathrm{Ps}}(\mathbf{t}) \equiv -\nabla_t^2 - \frac{1}{t}, \quad (5)$$

i.e.,

$$\langle \phi_a(\mathbf{t}) | H_{\mathrm{Ps}}(\mathbf{t}) | \phi_{a'}(\mathbf{t}) \rangle = E_a \delta_{aa'},$$
$$\langle \phi_a(\mathbf{t}) | \phi_{a'}(\mathbf{t}) \rangle = \delta_{aa'}. \quad (6)$$

The set consists of $1s$, $2s$, $\overline{3s}$ to $\overline{7s}$, $2p$, $\overline{3p}$ to $\overline{7p}$, $\overline{3d}$ to $\overline{7d}$, and $4f$ to $\overline{7f}$ states, where a "bar" distinguishes a pseudostate from an eigenstate. This set of 22 states has been used previously to investigate Ps scattering from H, He, and Ar [1,2,18,19] and is given explicitly in [19]. It derives from a set of H pseudostates, ψ_a, used earlier by van Wyngaarden and Walters [20] to study electron scattering by atomic hydrogen. The ϕ_a and ψ_a are related by

$$\phi_a(\mathbf{t}) = \frac{1}{\sqrt{8}} \psi_a\left(\frac{\mathbf{t}}{2}\right), \quad (7)$$

the energy E_a of ϕ_a [see Eq. (6)] being exactly one half of that of the corresponding ψ_a. The primary purpose of the pseudostates in the set ϕ_a is to represent the Ps continuum, in this case ionized states of H^- in which the detached electron has come under the influence of the projectile e^+. The pseudostates also take into account discrete states of Ps other than $1s$, $2s$, and $2p$.

For ψ^- we have used the approximation [13]

$$\psi^-(\mathbf{r}_1,\mathbf{r}_2) = N[\overline{\psi}(\mathbf{r}_1)\psi_0(\mathbf{r}_2) + \overline{\psi}(\mathbf{r}_2)\psi_0(\mathbf{r}_1)], \quad (8)$$

in which one of the two electrons is placed in the H($1s$) orbital ψ_0 while the other electron moves in a more diffuse s-state orbital $\overline{\psi}$ built out of a linear combination of the basis

$$r^n e^{-0.8r} \quad n = 0,1,\ldots,9. \quad (9)$$

The orbitals $\overline{\psi}$ and ψ_0 are not orthogonal and the normalization constant N is given by

$$N = 1/\sqrt{2(1+\langle \psi_0 | \overline{\psi} \rangle^2)}, \quad (10)$$

where we assume that $\overline{\psi}$ and ψ_0 are individually normalized. Determination of the coefficients of the basis (9) through application of the variational principle gives a binding energy of 0.362 eV, i.e., just less than one half of the exact H^- binding energy [10]. This is the best that can be expected from a split-shell function involving only s orbitals [21].

Finally, we note that the expansion (4) only permits the H atom in Eqs. (1) and (3) to be left in its $1s$ ground state, this is a restriction in our approximation. Amongst other things, this restriction rules out physical effects such as the van der Waals force in the Ps+H channels. It should also be observed that the expansion (4) is symmetric in the electron coordinates $\mathbf{r}_1$ and $\mathbf{r}_2$. Under the nonrelativistic Hamiltonian (11)/(12) the total electronic spin must be conserved, and since we consider a positron incident upon an electronic spin singlet state, i.e., H^-, we need only consider electronic spin singlet scattering. In this spin state the spatial part of the wave function must be symmetric under $\mathbf{r}_1 \leftrightarrow \mathbf{r}_2$ interchange.

The Hamiltonian for our collision system may be written

$$H = -\frac{1}{2}\nabla_p^2 + H_{\mathrm{H}^-}(\mathbf{r}_1,\mathbf{r}_2) + V_p(\mathbf{r}_p;\mathbf{r}_1,\mathbf{r}_2) \quad (11)$$

or equivalently,

$$H = -\frac{1}{4}\nabla_{R_1}^2 + H_{\mathrm{Ps}}(\mathbf{t}_1) + H_{\mathrm{H}}(\mathbf{r}_2) + V_{\mathrm{Ps}}(\mathbf{R}_1,\mathbf{t}_1;\mathbf{r}_2)$$
$$= -\frac{1}{4}\nabla_{R_2}^2 + H_{\mathrm{Ps}}(\mathbf{t}_2) + H_{\mathrm{H}}(\mathbf{r}_1) + V_{\mathrm{Ps}}(\mathbf{R}_2,\mathbf{t}_2;\mathbf{r}_1), \quad (12)$$

where

$$H_{\mathrm{H}^-}(\mathbf{r}_1,\mathbf{r}_2) \equiv -\frac{1}{2}\nabla_1^2 - \frac{1}{2}\nabla_2^2 - \frac{1}{r_1} - \frac{1}{r_2} + \frac{1}{|\mathbf{r}_1 - \mathbf{r}_2|} \quad (13)$$

is the H^- Hamiltonian,

$$V_p(\mathbf{r}_p;\mathbf{r}_1,\mathbf{r}_2) \equiv \frac{1}{r_p} - \frac{1}{|\mathbf{r}_p - \mathbf{r}_1|} - \frac{1}{|\mathbf{r}_p - \mathbf{r}_2|} \quad (14)$$

is the interaction between the e^+ and the H^-,

$$H_{\mathrm{H}}(\mathbf{r}) \equiv -\frac{1}{2}\nabla^2 - \frac{1}{r} \quad (15)$$

is the Hamiltonian for atomic hydrogen, and

$$V_{\rm Ps}(\mathbf{R},\mathbf{t};\mathbf{r}) \equiv \left(\frac{1}{\left|\mathbf{R}+\frac{1}{2}\mathbf{t}\right|} - \frac{1}{\left|\mathbf{R}+\frac{1}{2}\mathbf{t}-\mathbf{r}\right|} \right) - \left(\frac{1}{\left|\mathbf{R}-\frac{1}{2}\mathbf{t}\right|} - \frac{1}{\left|\mathbf{R}-\frac{1}{2}\mathbf{t}-\mathbf{r}\right|} \right) \tag{16}$$

is the interaction between the formed Ps and the residual H atom. Coupled equations for the functions F and G_a in Eq. (4) are obtained by substituting Eq. (4) into the Schrödinger equation and projecting with $\psi^-(\mathbf{r}_1,\mathbf{r}_2)$ and $\phi_a(\mathbf{t}_1)\psi_0(\mathbf{r}_2)$. These equations have the form

$$(\nabla_p^2+k_0^2)F(\mathbf{r}_p) = 2V(r_p)F(\mathbf{r}_p) + 4\sum_a \int K_a(\mathbf{r}_p,\mathbf{R}_1)G_a(\mathbf{R}_1)d\mathbf{R}_1,$$

$$(\nabla_{R_1}^2+p_a^2)G_a(\mathbf{R}_1) = 4\sum_{a'} U_{aa'}(\mathbf{R}_1)G_{a'}(\mathbf{R}_1) + 4\int K_a^*(\mathbf{r}_p,\mathbf{R}_1)F(\mathbf{r}_p)d\mathbf{r}_p + 4\sum_{a'} \int L_{aa'}(\mathbf{R}_1,\mathbf{R}_2)G_{a'}(\mathbf{R}_2)d\mathbf{R}_2, \tag{17}$$

where $\mathbf{k}_0$ is the momentum of the incident positron

$$\frac{k_0^2}{2}+\varepsilon^- = E = \frac{p_a^2}{4}+E_a+\varepsilon_0, \tag{18}$$

ε_0 (ε^-) is the energy of the H (H^-) state ψ_0 (ψ^-) and E is the total energy,

$$V(r_p) \equiv \langle \psi^-(\mathbf{r}_1,\mathbf{r}_2)|V_p(\mathbf{r}_p;\mathbf{r}_1,\mathbf{r}_2)|\psi^-(\mathbf{r}_1,\mathbf{r}_2)\rangle \tag{19}$$

is the static potential of the H^- ion,

$$U_{aa'}(\mathbf{R}_1) \equiv \langle \phi_a(\mathbf{t}_1)\psi_0(\mathbf{r}_2)|V_{Ps}(\mathbf{R}_1,\mathbf{t}_1;\mathbf{r}_2)|\phi_{a'}(\mathbf{t}_1)\psi_0(\mathbf{r}_2)\rangle \tag{20}$$

is the direct Coulomb interaction between the Ps and the H atom,

$$\int K_a(\mathbf{r}_p,\mathbf{R}_1)G_a(\mathbf{R}_1)\,d\mathbf{R}_1 = \int_{\text{fixed } \mathbf{r}_p} \psi^{-*}(\mathbf{r}_1,\mathbf{r}_2) \times (H-E)G_a(\mathbf{R}_1)\phi_a(\mathbf{t}_1)\psi_0(\mathbf{r}_2)d\mathbf{r}_1 d\mathbf{r}_2, \tag{21}$$

$$\int K_a^*(\mathbf{r}_p,\mathbf{R}_1)F(\mathbf{r}_p)d\mathbf{r}_p = \int_{\text{fixed } \mathbf{R}_1} \phi_a^*(\mathbf{t}_1)\psi_0^*(\mathbf{r}_2) \times (H-E)F(\mathbf{r}_p)\psi^-(\mathbf{r}_1,\mathbf{r}_2)d\mathbf{t}_1 d\mathbf{r}_2, \tag{22}$$

where * stands for complex conjugation, and

$$\int L_{aa'}(\mathbf{R}_1,\mathbf{R}_2)G_{a'}(\mathbf{R}_2)\,d\mathbf{R}_2 = \int_{\text{fixed } \mathbf{R}_1} \phi_a^*(\mathbf{t}_1)\psi_0^*(\mathbf{r}_2) \times (H-E)G_{a'}(\mathbf{R}_2)\phi_{a'}(\mathbf{t}_2)\psi_0(\mathbf{r}_1)d\mathbf{t}_1 d\mathbf{r}_2. \tag{23}$$

$K_a(\mathbf{r}_p,\mathbf{R}_1)$ is the Ps formation/destruction kernel, while $L_{aa'}(\mathbf{R}_1,\mathbf{R}_2)$ represents electron exchange between Ps and the H atom. Although our H^- state (8) is approximate, we use the exact H^- energy of 0.755 eV [10] for ε^- in Eq. (18), also in operating with the Hamiltonian H in Eqs. (21) and (22) we assume that, see Eq. (11),

$$H_{\mathrm{H}^-}\psi^-(\mathbf{r}_1,\mathbf{r}_2) = \varepsilon^-\psi^-(\mathbf{r}_1,\mathbf{r}_2), \tag{24}$$

where, again, ε^- has its exact value. The coupled Eqs. (17) are solved by conversion to partial-wave form, followed by application of the R-matrix technique [22,23]. Partial waves corresponding to total orbital angular momentum J from 0 to 20 are included in the calculations presented here.

The Eqs. (17) are solved subject to the boundary conditions

$$F(\mathbf{r}_p) \overset{r_p\to\infty}{\to} \left[1+\frac{\alpha^2}{i(k_0 r_p-\mathbf{k}_0\cdot\mathbf{r}_p)}\right] e^{i\mathbf{k}_0\cdot\mathbf{r}_p+i\alpha\ln(k_0 r_p-\mathbf{k}_0\cdot\mathbf{r}_p)} + f(\hat{\mathbf{r}}_p)\frac{e^{ik_0 r_p-i\alpha\ln(2k_0 r_p)}}{r_p}, \tag{25}$$

$$G_a(\mathbf{R}_1) \overset{R_1\to\infty}{\to} g_a(\hat{\mathbf{R}}_1)\frac{e^{ip_a R_1}}{R_1}, \tag{26}$$

where $\alpha=-1/k_0$ and unit vectors are indicated by a "hat." The form (25) represents the e^+ incident with momentum $\mathbf{k}_0$ in the Coulomb field of the H^- ion. In Eq. (26) Ps emerges in the state ϕ_a in the non-Coulombic field of the H atom. From Eqs. (25) and (26) the differential cross sections for elastic scattering and Ps formation are given by

$$\frac{d\sigma^{el}}{d\Omega} = |f|^2, \tag{27}$$

$$\frac{d\sigma_a^{Ps}}{d\Omega} = \frac{p_a}{2k_0}|g_a|^2. \tag{28}$$

We denote by σ^{el} and σ_a^{Ps} the corresponding integrated cross sections [24]. Because of the long-range character of the

Coulomb field, σ^{el} is in fact infinite. The ionization cross section, σ^{ion}, is calculated using the usual prescription [11,19,25,26]

$$\sigma^{ion}=\sum_a f_a\sigma_a^{\rm Ps}, \tag{29}$$

where f_a is the probability that the state ϕ_a overlaps the Ps continuum. The factor f_a is most conveniently calculated from

$$f_a=1-\sum_{nlm}|\langle\phi_{nlm}|\phi_a\rangle|^2, \tag{30}$$

where the sum is over all bound (orthonormal) eigenstates ϕ_{nlm} of Ps. For Ps formation in bound states other than $1s$, $2s$, or $2p$ (i.e., $n\geqslant 3$) we calculate an aggregate cross section, $\sigma_{n\geqslant 3}^{\rm Ps}$, from

$$\sigma_{n\geqslant 3}^{\rm Ps}=\sum_{\substack{a\\ a\neq 1s,2s,2p}}(1-f_a)\sigma_a^{\rm Ps}. \tag{31}$$

The binding energies of Ps($1s$) and Ps($n=2$) are 6.8 and 1.7 eV, respectively. Since they exceed the binding energy of H^- (0.755 eV), Ps formation in these states is exothermic, i.e., Ps can be formed at any impact energy. In the case of exothermic Ps formation in e^+ impact on neutral atoms it has been shown [27] that the Ps formation cross section becomes infinite as $1/k_0$ as $k_0\to 0$. The argument is simple. For exothermic formation $p_a\neq 0$ when $k_0=0$. In the limit $k_0\to 0$ the amplitude g_a becomes purely S wave, is nonsingular and, unless through some exceptional accident, nonzero. It then follows immediately from Eq. (28) that $\sigma_a^{\rm Ps}$ diverges as $1/k_0$. In the case of a negative ion, however, g_a becomes singular as $1/\sqrt{k_0}$ with the result that $\sigma_a^{\rm Ps}$ diverges as $1/k_0^2$. This point has been appreciated by Drachman [7,28]. That g_a diverges as $1/\sqrt{k_0}$ may be seen by examining the first-order perturbative approximation to Ps formation, i.e., the Coulomb-Born approximation. In this approximation [see Eqs. (12), (17), (18), (22), and (26)]

$$g_a=-\frac{1}{\pi}\int e^{-i\mathbf{p}_a\cdot\mathbf{R}_1}\phi_a^*(\mathbf{t}_1)\psi_0^*(\mathbf{r}_2)V_{\rm Ps}(\mathbf{R}_1,\mathbf{t}_1;\mathbf{r}_2)\times\chi_c(\mathbf{k}_0,\mathbf{r}_p)\psi^-(\mathbf{r}_1,\mathbf{r}_2)d\mathbf{R}_1d\mathbf{t}_1d\mathbf{r}_2, \tag{32}$$

where χ_c is the incident e^+ Coulomb wave [29]

$$\chi_c(\mathbf{k}_0,\mathbf{r}_p)=e^{-\pi\alpha/2}\Gamma(1+i\alpha)e^{i\mathbf{k}_0\cdot\mathbf{r}_p}\times{}_1F_1(-i\alpha;1;ik_0r_p-i\mathbf{k}_0\cdot\mathbf{r}_p). \tag{33}$$

In the limit $k_0\to 0$, the confluent hypergeometric function ${}_1F_1$ remains finite but the "density of states" factor $e^{-\pi\alpha/2}\Gamma(1+i\alpha)$ diverges as $1/\sqrt{k_0}$ [30]. An interesting difference on the case of a neutral atom is that this $1/\sqrt{k_0}$ divergence is present in every partial-wave contributing to Eq. (33) [29], consequently, the amplitude g_a does not become pure S wave in the limit $k_0\to 0$. Unlike the neutral atom situation, therefore the very low-energy differential cross section (28) is in general nonisotropic.

III. RESULTS

We present calculations in the impact energy range 0 to 10 eV. Our results for Ps formation are shown in Fig. 1. As indicated in the previous section, the exothermic cross sections for $1s$, $2s$, and $2p$ formation become infinite as $1/k_0^2$, or equivalently as $1/E_0$, as the impact energy $E_0=k_0^2/2$ tends to zero. At very low energies these cross sections may therefore be characterized as

$$\sigma_a^{\rm Ps}=\frac{A_a}{E_0}\pi a_0^2,\quad a=1s,2s,2p, \tag{34}$$

where we calculate that $A_{1s}=56.7$, $A_{2s}=71.5$, and $A_{2p}=265$ when E_0 is measured in electron volts. The limiting form (34) gives the calculated cross section correct to within 5% out to 1.4, 0.4, and 0.15 eV, respectively, for $1s$, $2s$, and

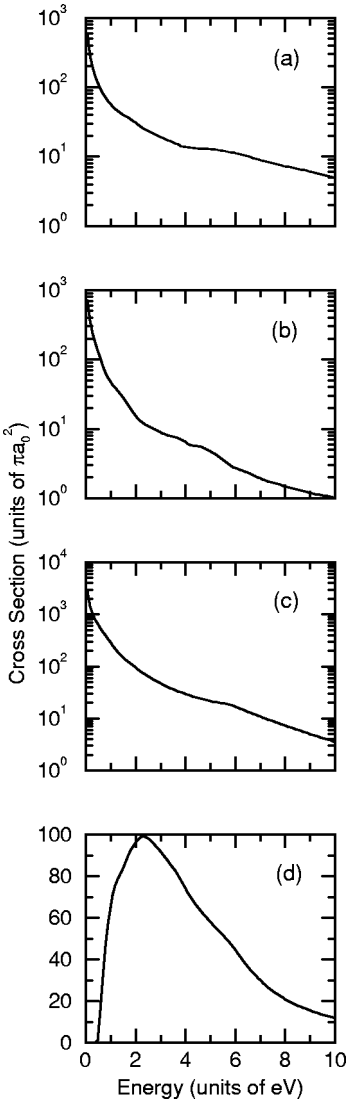

FIG. 1. Positronium formation cross sections: (a) Ps($1s$); (b) Ps($2s$); (c) Ps($2p$); (d) Ps($n\geqslant 3$).

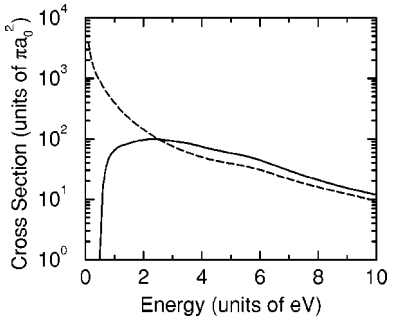

FIG. 2. Comparison of Ps formation cross sections: dashed curve, Ps($1s+2s+2p$); solid curve, Ps($n\geqslant 3$).

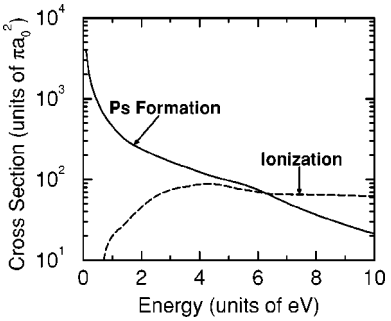

FIG. 3. Direct ionization and total Ps formation cross sections.

$2p$. It is clear from these numbers that the $2p$ formation cross section is by far the dominant one in the low-energy regime. However, with increasing impact energy the $1s$ cross section exhibits the slowest rate of fall with the result that it exceeds the $2s$ and $2p$ cross sections beyond 0.7 and 8.0 eV, respectively, being factors of 5 and 1.4 larger by 10 eV. The $2s$ cross section is everywhere smaller than the $2p$ cross section by a factor of roughly four.

Figure 1(d) shows an aggregate cross section, $\sigma^{\mathrm{Ps}}_{n\geqslant 3}$ for Ps formation into bound states with principle quantum number greater than two. This cross section has been extracted from the Ps pseudostates according to Eq. (31) and has a threshold at 0.49 eV corresponding to the lowest-energy pseudostate $(\overline{3p})$. It rises rapidly from threshold, reaching a maximum of 99 πa_0^2 at 2.3 eV, and subsequently declining to 11.9 πa_0^2 at 10 eV. Figure 2 compares $\sigma^{\mathrm{Ps}}_{n\geqslant 3}$ with the sum of the $1s$, $2s$, and $2p$ formation cross sections. Figure 2 also shows that Ps formation in states with $n\geqslant 3$ is dominant above 2.5 eV and at least up to 10 eV.

Despite the fact that Ps formation into the $1s$ ground state is not the dominant process at low energies, it is still of interest to compare our $1s$ results with the earlier calculations of Straton and Drachman [6]. This is done in Table I. Depending upon the approximation, they obtained a range of values differing by over a factor of 30. As Table I shows, their smallest values are still about 50% larger than what we have obtained here.

Let us now turn to direct ionization, the competing process to Ps formation above 0.755 eV. Figure 3 shows our calculated ionization cross section [see Eq. (29)]. In this figure it is compared with the total Ps formation cross section, i.e., the sum of the $1s$, $2s$, $2p$, and $n\geqslant 3$ Ps formation cross sections. We see that ionization begins to exceed Ps formation above 6.3 eV. Our calculated ionization cross section has a maximum of 88.6 πa_0^2 at 4.3 eV, which is over a factor of 2 larger than the maximum of the corresponding electron-impact cross section [14,31], this is consistent with our expectation of a stronger average e^+-target interaction than e^--target interaction, see Sec. I. A tabulation of our ionization cross section is given in Table II.

Besides integrated cross sections, there is some interest in differential cross sections for Ps formation [6,9]. In Figs. 4 to 6 we show a sample of our results for differential Ps formation in the $1s$, $2s$, and $2p$ states for e^+ impact energies of 0.1, 1.0, and 10.0 eV.

TABLE I. Ps($1s$) formation cross sections (πa_0^2).

Energy (eV)	Straton and Drachman [6] (range)	Present work
0.1	904–30 400	567
0.5	178–5760	116
1.0	82.5–2690	57

TABLE II. Direct ionization cross section, σ^{ion}, as calculated from Eq. (29).

Energy (eV)	Cross section (πa_0^2)
0.8	14.29
0.9	17.58
1.0	19.94
1.2	23.96
1.4	27.50
1.6	32.71
1.8	38.77
2.0	45.25
2.2	52.18
2.4	58.90
2.6	64.97
2.8	70.22
3.0	74.58
3.2	78.05
3.4	80.62
3.6	82.30
3.8	85.20
4.0	86.98
4.3	88.55
4.6	86.86
5.0	81.91
5.5	75.13
6.0	70.19
6.5	66.32
7.0	65.23
8.0	64.68
9.0	63.58
10.0	61.91

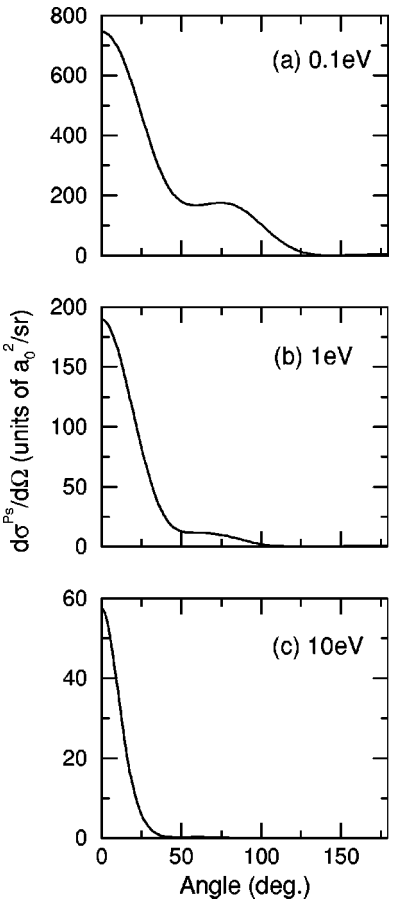

FIG. 4. Differential Ps($1s$) formation cross section.

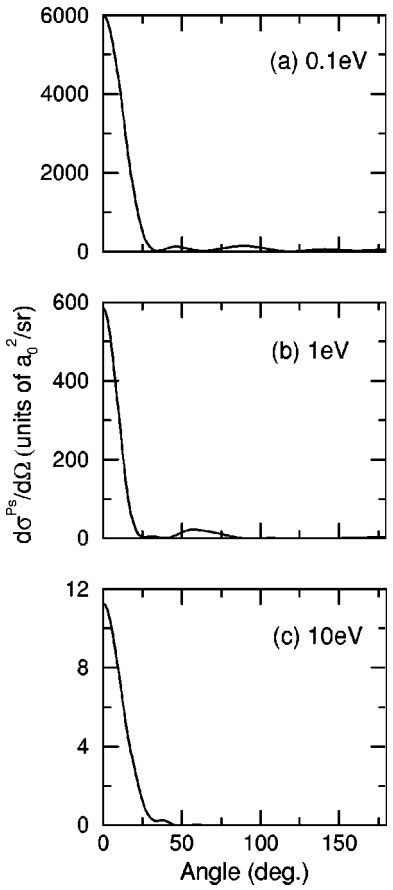

FIG. 5. Differential Ps($2s$) formation cross section.

Figure 4 exhibits the Ps($1s$) cross section. At all three energies this cross section is strongly forward peaked. At 0.1 and 1.0 eV there is a clear shoulder structure in the angular region 50° to 80° and a small but almost imperceptible rise towards 180°. This is different from the results of Straton and Drachman [6] at the same two energies which tend to show a dip near 70° and a much larger ratio of backward to forward scattering although the greatest scattering is still at the forward direction. At 0.1 and 1.0 eV our differential cross section is effectively negligible beyond 125° and 100°, respectively. By 10 eV, Fig. 4(c), the shoulder structure is no longer visible on the scale of our graph and the cross section is essentially confined to angles less than 40°.

The Ps($2s$) differential formation cross section, Fig. 5, is also strongly forward peaked and largely restricted to the angular range 0° to 30°, although there is some structure at larger angles. At 0.1 eV the forward $2s$ cross section is almost an order of magnitude larger than its $1s$ counterpart, Fig. 4(a), but by 10 eV is about five times smaller, Figs. 5(c) and 4(c), as we might expect from the relative sizes of the corresponding integrated cross sections at 10 eV.

Different from the others, the $2p$ cross section at 0.1 eV, Fig. 6(a), rises from the forward direction to a maximum of about 3000 a_0^2/sr at 20°, this is followed by secondary and tertiary maxima at 60° and 120°, respectively, and then a small rise towards the backward direction. By 1 eV, Fig. 6(b), like the others, the cross section is strongly forward peaked and the secondary maximum has now degenerated into a shoulder in the region 40° to 50°, with negligible undulatory structure at larger angles. By 10 eV, Fig. 6(c), we find a sharply peaked forward cross section similar to the $1s$ case, Fig. 4(c), but with a slightly higher forward cross section and a noticeably narrower peak.

The patterns seen in Figs. 4 to 6 are similar to what was obtained in the alkali metals [27], in particular the forward rise and 20° peak in the low-energy $2p$ cross section, Fig. 6(a).

It is also of interest to see how the individual partial waves contribute to Ps formation. In Table III, therefore, we list the partial-wave cross sections, $\sigma_a^{\mathrm{Ps}}(J,L)$, for $a=1s$, $2s$, and $2p$ formation at 0.1 eV. Here, J is the total orbital angular momentum and L is the orbital angular momentum of the outgoing Ps. The corresponding integrated cross section, σ_a^{Ps}, is given by

$$\sigma_a^{\mathrm{Ps}}=\sum_{J,L}\sigma_a^{\mathrm{Ps}}(J,L). \tag{35}$$

The table is truncated at values of J where the higher J cross sections are less than 0.1 πa_0^2. We see that Ps($1s$) formation is dominated by the $J=2$ wave (D wave) with lesser but comparable contributions from $J=1$ and 3. The $J=0$ (S wave) cross section is comparatively small, a pattern which we have grown used to seeing in ground-state Ps formation

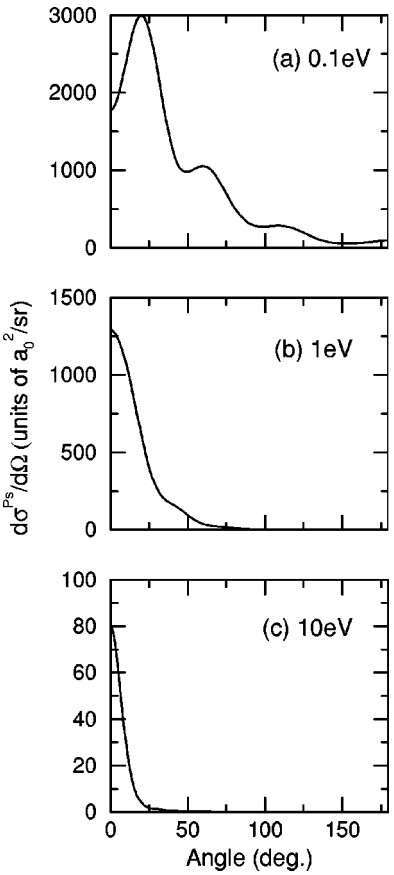

FIG. 6. Differential Ps($2p$) formation cross section.

[32] and which has been explained within the framework of the hidden crossing theory for e^+–H($1s$) scattering as being due to a destructive interference effect [33]. In the present context we note that this theory also explains the prominence of D-wave Ps formation in e^+–H($1s$) scattering as constructive interference. For Ps($2s$) formation the major contributions, of similar size, come from $J=2$, 3, and 5, with minima at $J=1$ and 4. For Ps($2p$) formation the dominant wave is $J=5$, $L=4$, closely followed by $J=4$, $L=3$, and further behind $J=6$, $L=5$; $J=1$, $L=0$, and $J=3$, $L=2$, in that order. Except for $J=2$, we see that

$$\sigma_{2p}^{\mathrm{Ps}}(J,L=J+1)<\sigma_{2p}^{\mathrm{Ps}}(J,L=J-1) \tag{36}$$

as we might expect from propensity. From the pattern of partial waves in Table III we might anticipate more structure than is seen in the differential cross sections of Figs. 4 to 6. Indeed, there is more structure, but on a comparatively negligible scale.

Drachman [28] has pointed out that near threshold $e^+ + \mathrm{H}^-$ cross sections might be estimated using quantum-defect theory from resonances in the Ps+H system which lie just below that threshold. Using the lowest S-wave resonance, which couples only to the Ps($1s$)+H($1s$) channel, he estimated an S-wave Ps($1s$) formation cross section of $(0.26\pm0.8)/k_0^2\ \ \pi a_0^2$. At $E_0=0.1$ eV, where our calculations indicate that the limiting form (34) still accurately applies, this gives an S-wave cross section of $(35\pm11)\ \ \pi a_0^2$, in excellent agreement with Table III. This is perhaps not surprising since the same approximation used in the present paper has also been applied to Ps+H scattering [1] where it gives a very good description of the Rydberg resonance structure converging onto the $e^+ + \mathrm{H}^-$ threshold, i.e., that structure is implicit in the present calculation.

TABLE III. Partial-wave cross sections for Ps($1s$), Ps($2s$), and Ps($2p$) formation at 0.1 eV.

(a) Ps($1s$)		
J	L	Cross section (πa_0^2)
0	0	36.1
1	1	122.3
2	2	282.8
3	3	103.9
4	4	20.0
5	5	1.5
6	6	0.3
(b) Ps($2s$)		
J	L	Cross section (πa_0^2)
0	0	43.7
1	1	24.7
2	2	186.2
3	3	163.3
4	4	46.6
5	5	183.4
6	6	64.4
7	7	2.5
(c) Ps($2p$)		
J	L	Cross section (πa_0^2)
0	1	13.0
1	0	200.6
1	2	37.0
2	1	58.8
2	3	71.7
3	2	166.1
3	4	85.9
4	3	719.9
4	5	11.1
5	4	865.1
5	6	5.6
6	5	417.2
6	7	0.4
7	6	47.7
7	8	0.0
8	7	1.5
8	9	0.0

IV. CONCLUSIONS

Using a relatively simple split shell wave function (8) for H^-, but treating it as if it were exact, Eq. (24), with the exact binding energy of 0.755 eV [10], we have calculated $1s$, $2s$, $2p$, and aggregate $n\geqslant3$ Ps formation cross sec-

tions, as well as the direct ionization cross section, for e^+ impact on H^- in the energy range 0 to 10 eV. For this purpose we have used a coupled pseudostate expansion where the pseudostates have all been centered on the e^+.

There are several obvious ways in which these calculations could be refined. First, and most obvious, would be the use of a highly accurate H^- target wave function, e.g., that of Pekeris [34]. Second, our treatment of ionization could be improved. Our approximation describes ionization as a charge-exchange process in which the loosely bound target electron is transferred into a continuum state of Ps. Such a representation, with a finite number of pseudostates, cannot be correct asymptotically in impact energy or angular momentum. Under these asymptotic conditions ionization is best described as a direct process with the ionized electron being centered on the target rather than the e^+. For these reasons we have confined ourselves to impact energies below 10 eV in the hope that nonasymptotic encounters of the e^+ with the H^-, where charge exchange is a more appropriate description of ionization, are dominant. Furthermore, as stated in Sec. I, our emphasis has been on Ps formation. In this context we have stressed the importance of allowing for the competition between Ps formation and ionization. However, this competition is restricted to the charge exchange regime where our present treatment of ionization should be satisfactory. Generally speaking, though, there is scope for further study of direct ionization as a process in its own right. A third refinement would be the removal of the assumption that the H atom is left in its ground state when H^- is ionized, either directly or through Ps formation, see Eqs. (1) and (3). Ps$(1s)$ and Ps$(n=2)$ formation with excitation of the atom to the $n=2$ state become possible at impact energies of 4.16 and 9.26 eV, respectively, direct ionization with H$(n=2)$ excitation starts at 10.96 eV.

The refinements outlined above will require further developmental work. It is not at all obvious that they will alter substantially the results presented in this paper, especially those for Ps formation. For the moment, the present paper represents a major advance in our knowledge of the e^+–H^- system.

ACKNOWLEDGMENT

This work was supported by EPSRC Grant Nos. GR/NO7424 and GR/MO1784.

[1] J. E. Blackwood, M. T. McAlinden, and H. R. J. Walters, Phys. Rev. A (to be published).

[2] C. P. Campbell, M. T. McAlinden, F. G. R. S. MacDonald, and H. R. J. Walters, Phys. Rev. Lett. **80**, 5097 (1998).

[3] H. R. J. Walters, J. E. Blackwood, and M. T. McAlinden, in *New Directions in Antimatter Chemistry and Physics*, edited by C. M. Surko and F. A. Gianturco (Kluwer, Dordrecht, 2001), p. 173.

[4] A. J. Garner, A. Özen, and G. Laricchia, Nucl. Instrum. Methods Phys. Res. B **143**, 155 (1998).

[5] R. J. Drachman, in *Positron Scattering in Gases*, edited by J. W. Humberston and M. R. C. McDowell (Plenum, New York, 1983), p. 203.

[6] J. C. Straton and R. J. Drachman, Phys. Rev. A **44**, 7335 (1991).

[7] R. J. Drachman, in *The Physics of Electronic and Atomic Collisions*, edited by Louis J. Dubi, J. Brian, A. Mitchell, J. William McConkey, and Chris E. Brion, AIP Conf. Proc. No. 360 (AIP, Woodbury, NY, 1995).

[8] L. H. Andersen, T. Andersen, and P. Hvelplund, Adv. At., Mol., Opt. Phys. **38**, 155 (1998).

[9] K. B. Choudhury, A. Mukherjee, and D. P. Sural, Phys. Rev. A **33**, 2358 (1986).

[10] A. M. Frolov and V. H. Smith, Jr., Phys. Rev. A **49**, 3580 (1994). We quote the H^- binding energy corresponding to an infinitely massive nucleus.

[11] A. A. Kernoghan, D. J. R. Robinson, M. T. McAlinden, and H. R. J. Walters, J. Phys. B **29**, 2089 (1996).

[12] H. R. J. Walters, A. A. Kernoghan, M. T. McAlinden, and C. P. Campbell, in *Photon and Electron Collisions with Atoms and Molecules*, edited by P. G. Burke and C. J. Joachain (Plenum, New York, 1997), p. 313.

[13] C. P. Campbell, M. T. McAlinden, A. A. Kernoghan, and H. R. J. Walters, Nucl. Instrum. Methods Phys. Res. B **143**, 41 (1998).

[14] F. Robicheaux, Phys. Rev. Lett. **82**, 707 (1999); Phys. Rev. A **60**, 1206 (1999). We note that the approximation used in these papers is in essence the same as that employed earlier by S. Lucey, C. T. Whelan, R. J. Allan, and H. R. J. Walters, J. Phys. B **29**, L489 (1996), in integral rather than partial-wave form, to study $(e,2e)$ collisions with H^-.

[15] In this paper we use atomic units (a.u.) in which $\hbar = m_e = e = 1$. The symbol a_0 denotes the Bohr radius.

[16] F. Robichaux, R. P. Wood, and C. H. Greene, Phys. Rev. A **49**, 1866 (1994).

[17] We have in fact performed some calculations using up to 27 H^- pseudostates of s, p, and d types, the results were unsatisfactory, suggesting very slow convergence.

[18] J. E. Blackwood, C. P. Campbell, M. T. McAlinden, and H. R. J. Walters, Phys. Rev. A **60**, 4454 (1999).

[19] M. T. McAlinden, F. G. R. S. MacDonald, and H. R. J. Walters, Can. J. Phys. **74**, 434 (1996).

[20] W. L. van Wyngaarden and H. R. J. Walters, J. Phys. B **19**, 929 (1986).

[21] H. S. W. Massey, *Negative Ions* (Cambridge University Press, Cambridge, 1976).

[22] C. P. Campbell, Ph.D. thesis, Queen's University Belfast, 1998.

[23] P. G. Burke and W. D. Robb, Adv. At. Mol. Phys. **11**, 143 (1975).

[24] In practice, all cross sections have been evaluated in partial-wave form.

[25] A. A. Kernoghan, M. T. McAlinden, and H. R. J. Walters, J. Phys. B **28**, 1079 (1995).

[26] I. Bray and A. T. Stelbovics, Phys. Rev. Lett. **70**, 746 (1993).
[27] M. T. McAlinden, A. A. Kernoghan, and H. R. J. Walters, Hyperfine Interact. **89**, 161 (1994).
[28] R. J. Drachman in *Atomic Physics with Positrons*, edited by J. W. Humberston and E. A. G. Armour (Plenum, New York, 1987), p. 203.
[29] N. F. Mott and H. S. W. Massey, *The Theory of Atomic Collisions* (Oxford University Press, Oxford, 1965).
[30] M. Abramowitz and I. A. Stegun, *Handbook of Mathematical Functions* (Dover, New York, 1972).
[31] L. Vejby-Christensen, D. Kella, D. Mathur, H. B. Pedersen, H. T. Schmidt, and L. H. Andersen, Phys. Rev. A **53**, 2371 (1996).
[32] C. J. Brown and J. W. Humberston, J. Phys. B **18**, L401 (1985); M. S. T. Watts and J. W. Humberston, *ibid.* **25**, L491 (1992); P. W. Van Reeth and J. W. Humberston, *ibid.* **30**, L95 (1997).
[33] S. J. Ward, J. H. Mocek, and S. Yu. Ovchinnikov, Phys. Rev. A **59**, 4418 (1999).
[34] C. L. Pekeris, Phys. Rev. **112**, 1649 (1958).